Nanoscale Res Lett (2009) 4:47–53
DOI 10.1007/s11671-008-9201-x

NANO EXPRESS

Synthesis of Indium Nanowires by Galvanic Displacement and Their Optical Properties

Haohua Li · Chaolun Liang · Meng Liu · Kuan Zhong · Yexiang Tong · Peng Liu · Greg A. Hope

Received: 10 August 2008 / Accepted: 22 October 2008 / Published online: 18 November 2008

Abstract Single crystalline indium nanowires were prepared on Zn substrate which had been treated in concentrated sulphuric acid by galvanic displacement in the 0.002 mol L^{-1} $In_2(SO_4)_3$-0.002 mol L^{-1} SeO_2-0.02 mol L^{-1} SDS-0.01 mol L^{-1} citric acid aqueous solution. The typical diameter of indium nanowires is 30 nm and most of the nanowires are over 30 μm in length. XRD, HRTEM, SAED and structural simulation clearly demonstrate that indium nanowires are single-crystalline with the tetragonal structure, the growth direction of the nanowires is along [100] facet. The UV-Vis absorption spectra showed that indium nanowires display typical transverse resonance of SPR properties. The surfactant (SDS) and the pretreatment of Zn substrate play an important role in the growth process. The mechanism of indium nanowires growth is the synergic effect of treated Zn substrate (hard template) and SDS (soft template).

H. Li · M. Liu · K. Zhong · Y. Tong (✉) · P. Liu (✉)
School of Chemistry and Chemical Engineering / MOE of Key Laboratory of Bioinorganic and Synthetic Chemistry, Sun Yat-Sen University, Guangzhou 510275, China
e-mail: cesdhx@mail.sysu.edu.cn

P. Liu
e-mail: pengliupd@hotmail.com

H. Li · M. Liu · K. Zhong · Y. Tong · P. Liu
Institute of Optoelectronic and Functional Composite Material, Sun Yat-Sen University, Guangzhou 510275, China

C. Liang
Instrumental Analysis & Research Center, Sun Yat-Sen University, Guangzhou 510275, China

G. A. Hope
School of Science, Griffith University, Nathan Qld 4111, Australia

Keywords Indium · Nanowire · Galvanic displacement · Surface plasmon resonance · Soft template

Introduction

The interaction of light with metal nanoparticles and nanowires as opposed to their bulk counterparts are subject to intense research for their application in plasmonics including chemical sensors and optical filters [1]. Some metal nanoparticles, such as gold and silver, have exhibited a strong absorption peak in the visible range of the spectrum, due to the excitation of a collective oscillation of electrons which is described as the surface plasmon resonance (SPR) [2–6]. However, nanorods and nanowires are the most prominent examples of nanoscale entities with SPR ranging from the visible to the near-infrared because the variation of the parameters such as shape and geometry enables tuning of the optical resonances [6–8]. Therefore, metal nanowires have received immense research intention in recent years owing to their tunable optical and electronic properties and potential applications in nanoelectronic, probes, biological sensors, storage media and sensing devices [9]. Gold and silver are among the most useful metals of the nanowires prepared for the purpose of optical resonances research [8, 10]. The nanowires based on the other metals Cu, Ni, Co have also been studied and they have also exhibited good SPR properties [7, 9, 11]. Further researches on the fabrication and their application of these prospective metal nanowires are of considerable importance nowadays. For example, indium nanowires exhibit excellent temperature-dependent electrical properties [12]. In particular, under the superconducting temperature, the electrical resistance of indium nanowires rapidly decreased, which are expected to play a part in making

magnetic field generators or superconducting quantum-interference devices [13]. Indium nanowire arrays on Silicon surface have been synthesized [14–18], the properties used as the temperature-induced metal-insulator transitions were studied. In addition, indium nanoparticles have also attracted particular interest because they can be used as lubricants, single electron transistors and tags for the detection of DNA hybridization [19–22].

The past studies on the preparation of indium nanowires using thermal evaporation have revealed the interesting structural and electrical and optical properties of these samples [15, 18, 23]. Galvanic displacement or the so-called immersion plating is another way to synthesize nanoscale materials in recent years [24]. It is a spontaneous electrochemical reaction induced by the difference in redox potentials between the substances of the solid substrates and the ions of the source materials. Obviously, it is different from electrodeposition and chemical bath deposition [25]; the substrates act as the reducing agents instead of the electric power or other reductant. Therefore, it yields the product with a high purity. On the other hand, it needs no apparatus as compared with the standard evaporation techniques [26]. Previous works on the synthesis of nanostructured materials via galvanic displacement have mainly focused on the metals including Au, Pd, Pt, Ag, Cu, Ni and Pb [24, 26–30], the binary intermetallic compounds such as Bi-Te [31], Pd-Ag and Pt-Ag [32].

In this paper, we report the synthesis of indium nanowires by galvanic displacement on a zinc sheet after being treated in concentrated sulphuric acid. The galvanic displacement is usually performed on a plain substrate, in this letter, we found that only nanoparticles grew on the untreated zinc sheets. However, indium nanowires can grow on the zinc sheet after being oxidized in concentrated sulphuric acid. The small holes in the porous ZnO oxide film formed on a treated zinc sheet play a confinement effect or act as a "template" in indium nanowires growth. This illustrates a simple way for the large-scale fabrication of indium nanowires with high purity at a mild condition. Furthermore, the structural characterization and UV properties of the as-prepared indium nanowires are also studied.

Experimental

Material

Zinc sheet (99.99%) was used as the substrate. The selenium dioxide, indium sulphate concentrated sulphuric acid (98%), citric acid, sodium dodecyl sulphonate (SDS), octyl hydride were analytical reagents. Trioctyl phosphine oxide (TOPO) was purchased from Alfa Aesar.

Synthesis of Indium Nanowires

The Zn sheet was polished and rinsed with acetone, and then it was put into the concentrated sulphuric acid and passivated for 6 h to form a porous oxide film. The passivated Zn sheet was immersed in the aqueous solution containing 0.002 mol L^{-1} $In_2(SO_4)_3$-0.002 mol L^{-1} SeO_2-0.02 mol L^{-1} SDS-0.01 mol L^{-1} citric acid aqueous solution without any disturbance for 40 min, SeO_2 was used as the supporting electrolyte in acid medium. The pH value of the solution was adjusted to be 1.4 by using 1 mol L^{-1} H_2SO_4. The deposits on the Zn sheet were analysed.

Characterization

The morphology of the as-prepared samples was observed by a field emission scanning electron microscope (FE-SEM, JSM 6330F, JEOL) and its structure was determined by a transmission electron microscope (TEM) and a high resolution-transmission electron microscope (HRTEM) (JEM 2010HR, JEOL) with an Oxford EDS spectrometer and an X-ray diffractometer (XRD, PW 1830, Philips).

The UV-vis Absorption Spectroscopy Measurement

The deposits were scraped down and dispersed in methanol and then sonicated for 1 h. The diameter of the nanowires suspended at the top of the solution is small and the diameter of the nanowires sinked at the bottom of the solution is large. So three different levels from top to bottom of the dispersion were collected. Each part of the dispersion was centrifugated for 20 min. The precipitations were redispersed in octane-TOPO solution and sonicated for 10 min, respectively, as illustrated by the literature [30]. The UV-vis absorption spectroscopy of these nanowires with different diameters was measured by a UV-visible Spectrophotometer (UV-vis UV-2501PC, Shimadzu). The average diameter and aspect ratio of the nanowires dispersed in different levels were calculated by SEM images.

Results and Discussion

Figure 1 presents the XRD pattern of the as-deposited sample. The diffraction peaks ($2\theta = 36.5$, 39.2 and 43.4) belong to the zinc substrate. While the diffraction peaks ($2\theta = 33.1$ and 54.6) belong to the (101) and (112) facets of indium with tetragonal structure (JCPDS Card 05-0642). The XRD results indicate that the as-deposited sample is tetragonal phase indium.

Figure 2 is the typical SEM images of the as-prepared samples. The SEM image at a low magnification (as shown

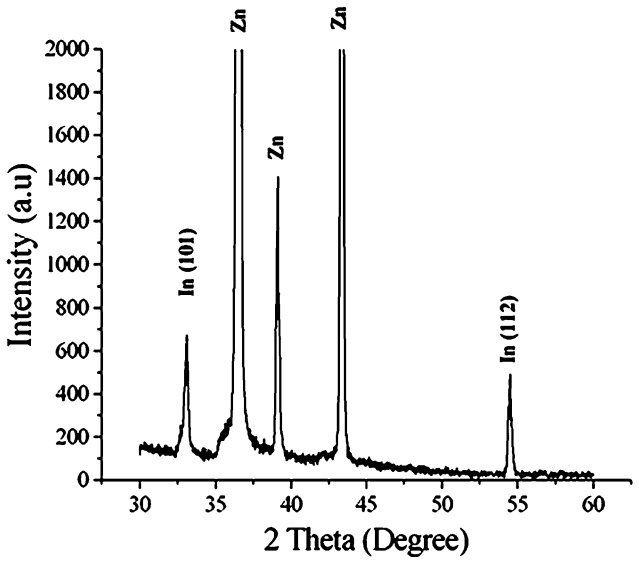

Fig. 1 X-ray diffraction patterns of the as-deposited sample

in Fig. 2a) clearly reveals the film consists of a high yield of nanowires. Most of the nanowires are over 30 μm in length. Figure 2b depicts the detail morphology of the nanowires. The average diameter of indium naowires is about 30 nm and the diameter ranges from 20 nm to 60 nm.

The microstructure of individual nanowire was further investigated by TEM and HRTEM. Figure 3 shows a typical TEM image of the sample after ultrasonic treatment, a fragment of indium nanowires was captured. The diameter of the nanowire is about 25 nm. The inset in Fig. 3 shows the selected area electron diffraction (SAED) pattern of the circled area in Fig. 3 taken along [001] zone axis. In the SEAD pattern, sharp and clear diffraction spots were observed, proving that the nanowire is single crystalline. The reflections correspond to (110), $(1\bar{1}0)$ and (200) lattice planes of In with tetragonal structure. Therefore, the In nanowire adopt a single crystalline structure with tetragonal phase. From the SAED, it can also be found that the growth direction of this nanowire is along [100] direction.

The corresponding high resolution transmission electron microscopy is shown in Fig. 4, the area in which lattice fringe image appeared reveals the orientation, size and grain boundary of the nanowires. In order to investigate the details of the crystal structure, Fouier filtered reconstructed image is shown in Fig. 5. From the image, two-dimensional lattice fringes were observed in the individual indium nanowire. The marked d spacing of 0.25 nm meeting at an angle of 90^0 corresponds to the interplanar distance of (110). In addition, the planes with an interplanar distance of 0.16 nm can be indexed as (200). In other words, the indium nanowire was formed by the stacking of (100) planes, which indicates that the indium nanowire grew along a-axis of the tetragonal lattice.

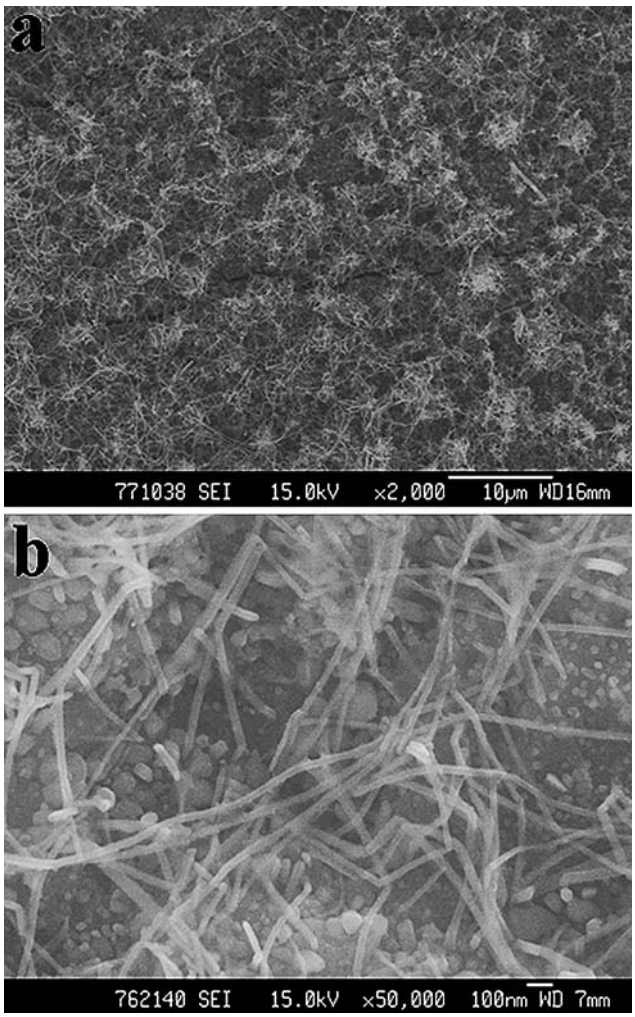

Fig. 2 The typical SEM images of the as-prepared nanowires. **a**, at a low magnification. **b** at a high magnification

To further demonstrate the structure and growth direction of In nanowire, simulation of the perfect tetragonal In crystal with electron beam along [001] direction was carried out by Jems program. As is shown in Fig. 6b, periodicity and contrast of the simulation image (the inset) were in good agreement with that of the experimental image. A structural model of body-centred tetragonal indium unit cell along [001] is depicted in Fig. 6a. Based on this structure, simulation image indicates that around the Scherzer defocus, the location of indium columns is represented by the dark contrast, while the bright dots represent the vacancy among the atomic columns. The dark spheres show the stacking sequence of (100) planes of indium. The HRTEM images and simulation results reveal that the dark contrast areas correspond to atomic columns and the In nanowire consisted of the stacking of (100) planes.

The size-dependent optical properties were investigated. The as-prepared samples were dispersed in methanol.

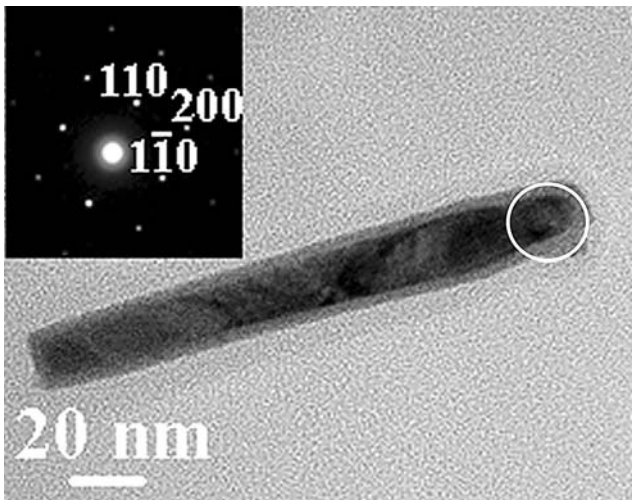

Fig. 3 TEM image of In nanowire and the SEAD pattern of the circled area in TEM image.The HRTEM image of the nanowire is shown in Fig. 4, the lattice fringe image can be observed, this reveals the orientation, size and grain boundary of the nanowire

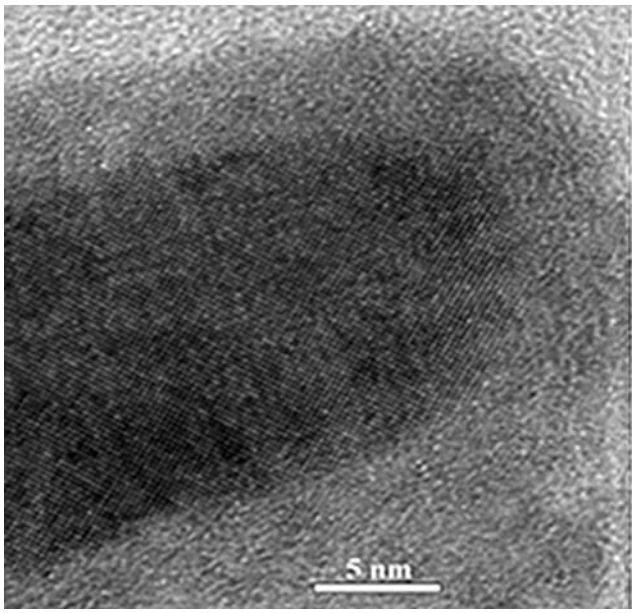

Fig. 4 HRTEM image of the In nanowire

Generally, the size of the nanowires dispersed in methanol solution increases from top to bottom. The nanowires in different levels of the methanol dispersion solution were extracted. Fig. 7 presents the absorption spectra of indium nanowires with different diameters in octane-TOPO solution, the average diameter and aspect ratio of the nanowires were 40 nm and 10:1 (top); 105 nm and 7:1 (middle) and 300 nm and 5:1 (bottom), respectively. It can be seen that the absorption peak of nanowires with small diameter appeared at 525 nm, the peak of the nanowires

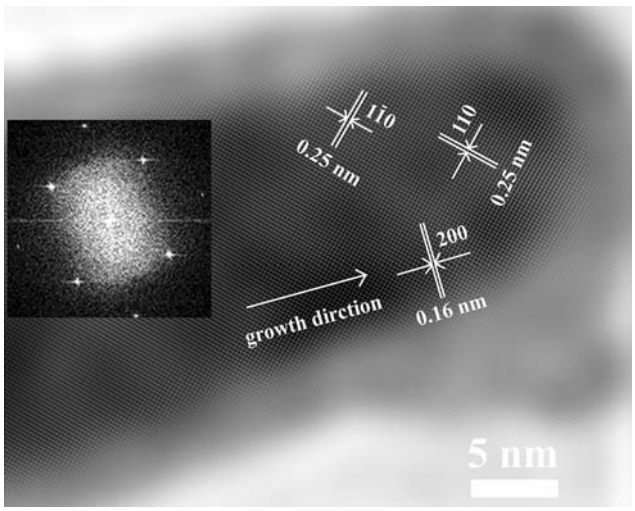

Fig. 5 The diffractogram of Fig. 4 (inset) and its Fouier filtered reconstructed image

with middle diameter appeared at 551 nm and the peak of nanowires with large diameter appeared at 559 nm. Therefore, a red shift of the maximum absorption wavelength can be observed with the decrease of the aspect ratio. The light absorption is due to collective resonant absorption of free electrons at the surface of particles. Thus, the overall UV-vis absorbance of the one-dimensional (1-D) nano-structures, such as nanowires, nanorods and even the elongated ellipsoids, is the summation over the three dimensions in which plasmon oscillation is not prohibited. According to Gans theory [6], for 1-D nano-structures, the direction of the plasmon oscillation depends on the orientation of nanowires with respect to the wave-vector of incident light, which can lead to two absorbance peaks including transverse resonance (shorter wavelength) and longitudinal resonance (longer wavelength). Furthermore, Gans theoretically deduced the equation between the extinction coefficient γ and the wavelength λ by using dipole approximation. The relation between γ and λ is significantly affected by the aspect ratio. A term geometrical factor P_j which corresponds to three dimensional axes A, B and C was introduced to calculate the absorbance of light in Gans equation. For 1-D nano-structures, the B and C axes (transverse direction) are equal and correspond to the diameter and the A-axis (longitudinal direction) represents the length. The screening parameter R_j is defined as $(1\text{-}P_j)/P_j$, R_j strongly depends on the anisotropy of the samples. With increasing aspect ratio, the screening parameter R_A (the longitudinal oscillation) shifts towards infinity, while R_B and R_C (transverse plasmon oscillation) reaches 1. The calculation shows that the maximum of the longitudinal absorbance band shifts to longer wavelengths and the transverse resonance maximum slightly shifts to shorter wavelengths with increasing aspect ratio. Both

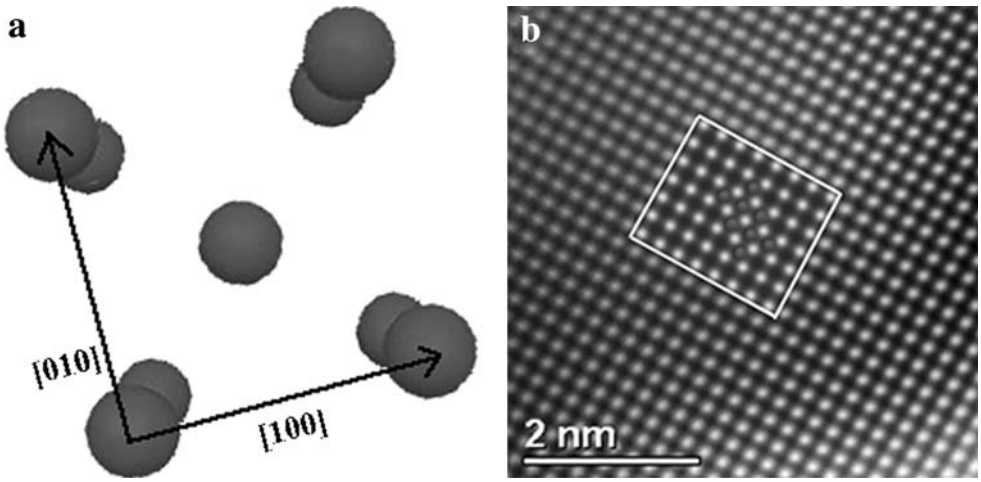

Fig. 6 **a**, A structure model of body-centred tetragonal indium along [001] zone axis. **b** Enlarged IFFT image. Image simulation (the inset) is compared with the experimental image. Multislice method was performed for the calculation. The dark spheres of inset image show the stacking model of indium atomic columns

shifts can be attributed to the change in the screening parameter [6].

In Fig. 7, it can also be found that only one absorption peak near 525 to 559 nm was observed and the peaks shifted to longer wavelength with the decrease of the aspect ratio; therefore, these peaks should be caused by the transverse resonance of the nanowires. However, the absorption band caused by longitudinal resonance is absent in Fig. 7. This may be due to the low dielectric constant of octane (2.1–2.3, 20°C). Because of the lower dielectric constant, the screening of electrical dipole decreases and the longitudinal resonance peak disappears [9]. On the other hand, in the past years many studies focused on the SPR of indium nanoparticles, the peak wavelength existed in the range from 240 nm to 400 nm [21–24, 33], this is

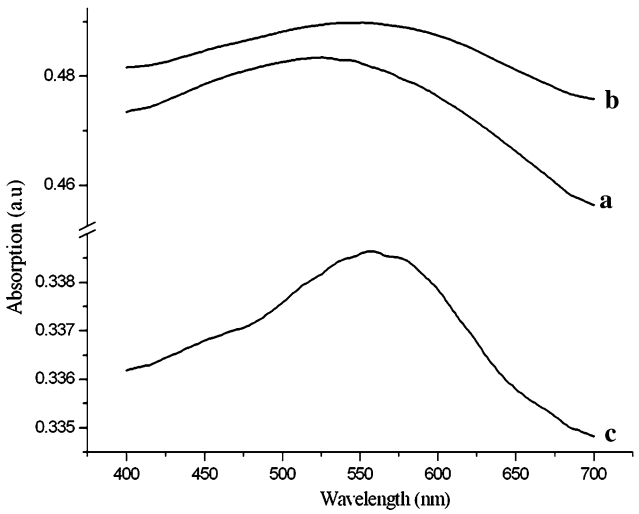

Fig. 7 UV-vis absorption spectrum of In nanowires with different diameters in octane-TOPO solution. **a**, The nanowires extracted from the top level of methanol dispersion solution. **b**, The nanowires extracted from the middle level of methanol dispersion solution. **c** The nanowires extracted from the bottom level of methanol dispersion solution

different from the SPR of In nanowires mentioned above. In this work, the wavelength shifted to longer wavelength because indium nanowires other than indium nanoparticles are dispersed in octane/TOPO solution. However, it is difficult to compare these data because the SPR is solvent and morphology dependent [34].

In our experiments, we found that the surfactant (SDS) played an important role in the indium nanowires growth. Some large particles instead of nanowires were formed on the treated Zn substrate if SDS was not added into the solution. In nanowires can grow on the substrate only when SDS was added. At the beginning of the reaction, the In^{3+} ions attacked Zn atoms and were reduced to be In atoms. The small In crystalline seeds formed on the surface of Zn substrate. The surfactant, SDS, was adsorbed around the In crystalline seeds, while SDS is a anionic surfactant and In^{3+} ions were apt to be attracted. According to the HRTEM image and SAED experiments, the growth direction of In nanowires is along (100) facets; therefore, it can be deduced that a preferential adsorption of SDS on the (100) facets of In seeds occurred. In^{3+} ions obtained electrons which was transferred by In atoms from Zn substrate and piled alone (100) facets. In this case, SDS acted as a soft template for the growth of In nanowires.

On the other hand, we also found that In nanowires could not grow on the Zn substrate which was not treated in concentrated sulphuric acid even if there was SDS in the solution.

Figure 8 is the SEM image of the Zn substrate after treated in concentrated sulphuric acid. The substrate was eroded by concentrated sulphuric acid and the oxide film formed. It can be seen that the oxide film distributed many small holes with the diameter ranged from 200 to 1000 nm in Fig. 8. These holes acted as a "hard template" for the growth of In nanowires. On the surface of the untreated plane Zn substrate, the replacement reaction can take place anywhere on the substrate and In atoms deposited and

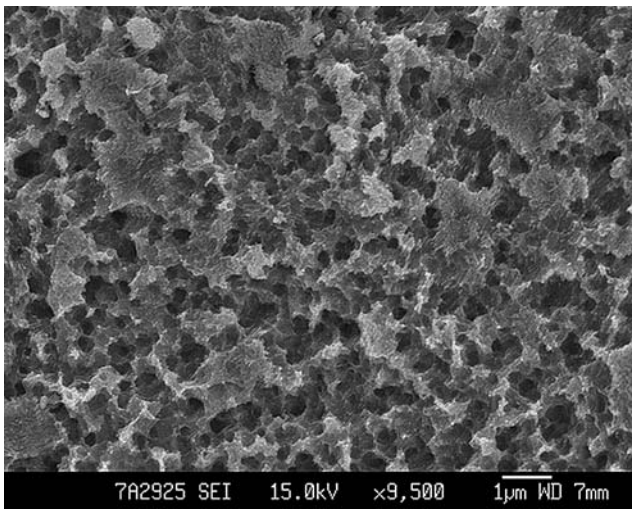

Fig. 8 The SEM image of Zn substrate after treated in concentrated sulphuric acid for 6.5 h

spreaded out along two-dimensional space on the whole surface. In fact, large particles of In deposit can be observed on the untreated Zn substrate in our experiment. After treatment with concentrated sulphuric acid, there are many holes formed on the surface of Zn substrate, the surfactant SDS was absorbed on the inner surface of the small holes and the anionic surfactant SDS could further attract In^{3+} ions, In^{3+} ions contacted Zn atoms at the bottom of the hole (Zn Substrate) and were reduced to In atoms. The size of the crystalline seeds was confined by the "hard template". Then SDS were preferentially adsorbed on the (100) facets. Hence, the growth of In nanowires was the synergic effect of treated Zn substrate and SDS.

Conclusion

In summary, high purity single crystalline indium nanowires can be prepared on Zn substrate via galvanic displacement at room temperature. These indium nanowires exhibit the expected SPR properties. The mechanism of the growth of indium nanowires is the synergic effect of treated Zn substrate (hard template) and SDS (soft template).

Acknowledgments This work was supported by the National Foundations of China-Australia Special Fund for Scientific and Technological Cooperation (grant No. 20711120186), the Natural Science Foundations of China (grant No. 20573136), the Natural Science Foundations of Guangdong Province (grant No. 8151027501000095).

References

1. A. Bouhelier, R. Bacgelot, J.S. Im, G.P. Wiederrecht, G. Lerondel, S. Kostcheev, P. Royer, J. Phy, Chem Br **109**, 3195 (2005)
2. S.A. Dong, S.P. Zhou, Mater Sci Eng B **140**, 153 (2007). doi:10.1016/j.mseb.2007.03.020
3. A.P. Zhang, Y. Fang, Chem. Phys. **332**, 284 (2007). doi:10.1016/j.chemphys.2006.12.013
4. Y.P. Bi, G.X. Lu, Chem Mater **20**, 1224 (2008). doi:10.1021/cm703093m
5. L.A. Sweatlock, S.A. Maier, H.A. Atwater, J.J. Penninkhof, A. Polman, Phys. Rev. B. **71**, 235408/1 (2005)
6. B.M. Van der Zande, M.R. Bohmer, L.G. Fokkink, C. Schoenenberger, Langmuir **16**, 451 (2000). doi:10.1021/la9900425
7. G.M. Sando, A.D. Berry, A.D. Owrutsky, J.C Owrusky, J. Chem. Phys. **127,** 074705/1 (2007)
8. S. Navaladian, C.M. Janet, B. Viswanathan, T.K. Varadarajan, R.P. Viswanath, J Phys Chem C **111**, 14150 (2007). doi:10.1021/jp0744782
9. A. Azarian, Z.A. Iraji, A. Dolati, Opt. Commun. **274**, 471 (2007). doi:10.1016/j.optcom.2007.02.031
10. Q.Q. Wang, J.B. Han, H.M. Gong, D.J. Chen, X.J. Zhao, J.Y. Feng, J.J. Ren, Adv Funct Mater **16**, 2405 (2006). doi:10.1002/adfm.200600096
11. R.L. Zong, J. Zhou, B. Li, M. Fu, S.K Shi, L.T Li, J. Chem. Phys. **123,** 094710/1 (2005)
12. S.S. Oh, D.H. Kim, M.W. Moon, A. Vaziri, M. Kim, E. Yoon, K.H. Oh, J.W. Hutchinson, Adv Mater **20**, 1093 (2008). doi:10.1002/adma.200702134
13. N. Giordano, Phys. Rev. Lett. **61**, 2137 (1988). doi:10.1103/PhysRevLett.61.2137
14. J.R. Ahn, J.H. Byun, J.K. Kim, H.W. Yeom, Phys. Rev. B. **75,** 033313/1 (2007)
15. K. Fleischer, S. Chandola, N. Esser, W. Richter, J.F. Mcgilp, W.G. Schmidt, S. Wang, W. Lu, J. Bernholc, Appl Surf Sci **234**, 302 (2004). doi:10.1016/j.apsusc.2004.05.114
16. S. Wippermann, W.G. Schmidt, A. Calzolari, M.B. Nardelli, A.A. Stekolnikov, K. Seino, F. Bechstedt, Surf. Sci. **601**, 4045 (2007). doi:10.1016/j.susc.2007.04.053
17. A.A. Stekolnikov, K. Seino, F. Bechstedt, S. Wippermann, W.G. Schmidt, A. Nardelli, M. Buongiorno, Phy. Rev. Lett. **98**, 26105/1 (2007)
18. J.L. Li, X.J. Liang, J.F. Jia, X. Liu, J.Z. Wang, E.G. Wang, Q.K. Xue, Appl Phys Lett **79**, 2826 (2001). doi:10.1063/1.1413722
19. Y.B. Zhao, Z.J. Zhang, H.X. Dang, J Phys Chem B **107**, 7574 (2003). doi:10.1021/jp027768l
20. K. Hitzbleck, H. Wiggers, P. Roth, Appl. Phys. Lett. **87**, 093105/1 (2005)
21. H. Yu, P.C. Gibbons, K.F. Kelton, W.E. Buhro, J. Am. Chem. Soc. **123**, 9198 (2001). doi:10.1021/ja016529t
22. F.Y. Wu, C.C. Yang, C.M. Wu, C.W. Wang, W.H. Li, J.Appl. Phys. **101,** 09G111/1 (2007)
23. C.G. Hwang, N.D. Kim, S.Y. Shin, J.W. Chung, N J Phys **9**, 1367 (2007). doi:10.1088/1367-2630/9/8/249
24. C. Carraro, R. Maboundian, L. Magagin, Surf Sci Rep **62**, 499 (2007). doi:10.1016/j.surfrep.2007.08.002
25. G. Hodes, Phys Chem Chem Phys **9**, 2181 (2007). doi:10.1039/b616684a
26. M. Aizawa, A.M. Cooper, M. Malac, J.M. Buriak, Nano Lett **5**, 815 (2005). doi:10.1021/nl048008k
27. M.H. Nezhad, M. Aizawa, L.J. Porter, A. Ribbe, J. Buriak, Small **1**, 1076 (2005). doi:10.1002/smll.200500121
28. Y.G. Sun, B. Mayer, Y.N. Xia, Adv Mater **15**, 641 (2003). doi:10.1002/adma.200301639
29. Y.G. Sun, B. Mayer, Y.N. Xia, Nano Lett **2**, 481 (2003). doi:10.1021/nl025531v
30. C.Y. Wang, M.Y. Lu, H.C. Chen, L.J. Chen, J Phys Chem C **111**, 6215 (2007). doi:10.1021/jp068662j
31. F. Xiao, B. Yoo, K.H. Lee, N.V. Myung, J. Am. Chem. Soc. **129**, 10068 (2007). doi:10.1021/ja073032w

32. J.Y. Chen, B. Wiley, J. Mclellan, Y.J. Xiong, Z.Y. Li, Y.N. Xia, Nano Lett **5**, 2058 (2005). doi:10.1021/nl051652u
33. N.H. Chou, X.L. Ke, P. Schiffer, R. Schaak, J. Am. Chem. Soc. **130**, 8140 (2008). doi:10.1021/ja801949c
34. R.A. Raneev, A.I. Ryasnyanskiy, U. Chakravarty, P.A. Naik, H. Srivastava, M.K. Tiwari, P.D. Gupta, Appl Phys B **86**, 337 (2007). doi:10.1007/s00340-006-2526-1